NSG-5062

Institute for Physical Science and Technology

University of Maryland
College Park, MD 20742

Technical Note BN-871 December 1977

ATMOSPHERIC LIDAR RESEARCH APPLYING TO H_2O, O_2 AND AEROSOLS

by

T. J. McIlrath and T. D. Wilkerson

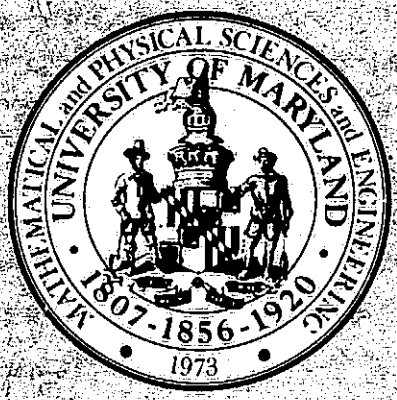

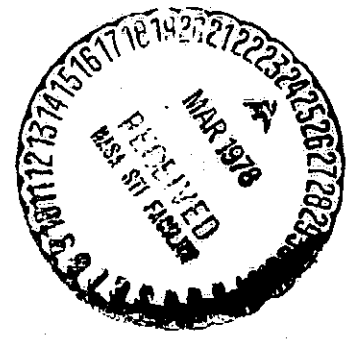

ATMOSPHERIC LIDAR RESEARCH

APPLYING TO H_2O, O_2 AND AEROSOLS

Final report on research

carried out under NASA grant

NSG-5062 (Sup. 1)

by

T. J. McIlrath and T. D. Wilkerson

Institute for Physical Science and Technology

University of Maryland, College Park, Maryland 20742

(301) 454-2702

December, 1977

Table of Contents

Abstract

Experimental research on a near infrared tunable dye laser is reported, and theoretical simulations are presented for various lidar configurations. The visible and near-IR wavelengths considered (420-960 nm) are suitable for observations of aerosols, water vapor, molecular oxygen pressure and temperature in the troposphere and above. The first phase of development work is described on a ruby-pumped, tunable dye laser for the wavelength region 715-740 nm. Lidar simulations are summarized for measurements of H_2O (~ 720 and 940 nm) and for "two color" lidar observations of aerosols in the atmosphere.

1. Introduction

Remote sensing of the environment by means of laser radar (lidar) is becoming a practical reality. Recent contributions to this effort by a research group at the University of Maryland are summarized here. This work was supported by NSG 5062 (Sup. 1) to accelerate the application of lidar to meteorological and climatological observations.

Experimental research on a near infrared tunable dye laser is reported, and theoretical simulations are presented for various lidar configurations. The visible and near-IR wavelengths considered (420-960 nm) are suitable for observations of aerosols, water vapor, molecular oxygen pressure and temperature in the troposphere and above.

Lidar appears workable from a variety of platforms including the Space Shuttle. It is hoped that the research contributions reported here are useful advances towards a long range collaboration with NASA on the environmental applications of lidar systems.

Section 2 summarizes the first phase of developmental work on a ruby-pumped, tunable dye laser for the wavelength region 715-740 nm. When run narrow band, this laser is the starting point for a lidar probe of water vapor structure in the atmosphere, and for pressure and temperature soundings using the A-bands of O_2.

Section 3 summarizes the lidar simulations carried out for measurements of H_2O (~ 720 and 940 nm) and for "two color" lidar observations of aerosols in the atmosphere. The applications range from marine boundary layer problems of interest to the Navy to stratospheric assay of H_2O for its role in stratospheric chemistry and transport.

2. Tunable, Near Infrared Dye Laser

This section describes the tunable dye laser constructed under NSG 5062, and summarizes the operating parameters of that laser. It is a frequency-tunable dye laser operating in the near infrared, pumped by a giant-pulse ruby laser. The output wavelength is variable from 715-740 nm with the existing optical elements and dye solution. This range may be extended to 800 nm by an appropriate substitution of dye, whereas outputs as far as 1μ should be obtainable by additional changes in dye and cavity optics. The narrow-band spectral output is a single line of width 0.08 nm (FWHM), with a beam divergence of less than 2 milliradians. With this system we achieved a peak conversion efficiency of 5% from ruby pump light into tunable narrow-band output at an output energy of 20 millijoules. The ruby pump beam has a risetime of 15 ns and a pulse width of 30 ns (FWHM), and the temporal behavior of the dye laser is similar.

The dye laser system consisting of laser cavity, alignment optics, and dye circulating system is constructed on a 2' x 4' optical breadboard, making the system readily portable. The laser cavity consists of a dye cell, an output reflector, an echelle grating used as a dispersive rear reflector, an intracavity beam expander, and a cavity aperture. A helium-neon alignment laser and its associated beam-steering mirrors are included as integral parts of the cavity layout, as are beam-steering optics for the ruby pump beam.

Associated with the dye cell is a circulating system consisting of a variable-speed dye pump, reservoir, filter, and filling valves. This system maintains a continuous circulation of dye to prevent formation of thermal gradients and accumulation of reaction products in the dye cell. In addition the 5μ Teflon filter serves to remove reaction products and particulates from

the dye solution. Because of the chemically reactive nature of the dye solvent DMSO, the circulating system components were chosen to place only stainless steel and Teflon in contact with the dye solution.

The dye used in this work is Kodak #7663, known as DTDC, or 3-Ethyl-2-[5-(3-ethyl-2-benzothiazolinylidene) - 1,3 - pentadienyl] benzothiazolium Iodide (M.W. 518.48), and belongs to the family of cyanine dyes which span the near infrared in their capacity as laser dyes. In this application the solvent dimethyl sulfoxide (DMSO) provides the optimum lasing efficiency over the region 7150-7400 Å. Appendix 1 discusses practical considerations which arise in the use of the DTDC-DMSO combination as a laser dye solution.

In order to provide control over mode structure, a fairly thin (5 mm) dye cell is used. This enables pumping of a small volume of dye. A concentrated (5×10^{-4}M) dye solution is required for adequate gain.

The major thrust of the work has involved variations in cavity configuration which affect the spectral output and beam divergence. We have examined controlling the cavity diameter and the use of an intracavity beam expander as two ways of affecting these output parameters. We have seen, for example, that in a 35 cm long cavity consisting of a grating, aperture, dye cell, and front reflector, the spectral width decreases from 0.25 nm to 0.08 nm when the aperture is reduced from 7 mm to 2 mm. At the same time the divergence changes from 5 mr vertically (in the dispersion plane of the grating) and 3 mr horizontally to within 2 mr in both dimensions. The reduction to a 2 mm aperture proves undesirable however, in that it reduces the output pulse energy from 20 millijoules to about one millijoule, with poor shot-to-shot stability, despite adjustments in dye concentration to ameliorate this. As a consequence we were unable to obtain adequate lasing with the beam expander also inserted between the dye cell and the grating, since in

this configuration the expander's 2 mm-diameter diverging lens faced the dye cell, rendering only a 2-mm diameter region of dye useful for lasing.

A greater measure of success was achieved by inserting the beam expander between the dye cell and the output mirror such that its 1 cm diameter converging lens faced the dye cell. Since this configuration enabled the pumping of a larger volume of dye, the output energy was consequently higher. Using the expander in this way without any additional cavity aperture provided 20 millijoule pulses of 0.25 nm width, while additionally inserting a 7 mm aperture between the grating and the dye cell narrowed the output linewidth to 0.08 nm, with pulse energies of 13 millijoules. The divergence of the beam in this configuration was not studied in detail, but it appeared to be at least as good as the case where the 7 mm aperture was used without a beam expander; i.e., within 3 mr.

Future work on this dye laser can follow two lines of development. The first path involves narrowing the spectral width of the dye laser output by the use of one or more intracavity Fabry-Perot etalons. By using an appropriate set of plate spacings in the etalons, a spectral width on the order of 10^{-3} nm may be obtained. The etalons may be angle-tuned or pressure-tuned to vary the output wavelength. The second line of development concerns the total energy output of the dye laser. This can be increased by the addition of one or more single-pass amplifier dye cells external to the existing dye laser cavity. These cells, as well as the existing oscillator dye cell, would all be pumped by a portion of the same ruby pulse, although the optical path length for these various pump beams must be adjusted for oscillator-amplifier synchronization.

3. Lidar Simulations

Detailed numerical simulations of lidar performance are summarized here for three categories of measurement:

A. $[H_2O]$ profiles (vertical and horizontal) seen from a lidar station at sea level, $\lambda \sim 720$ nm

B $[H_2O]$ profiles (vertical) seen from platforms at 20, 30 and 200 km altitude, $\lambda \sim 940$ nm

C. Aerosol profiles (vertical) observed from 200 km altitude with "two color" lidars (694/347 nm; 850/425 nm)

Appendix 2 contains short papers given on these subjects at a Navy workshop on Remote Sensing of the Marine Boundary Layer, Vail, CO (August, 1976) and the Eighth International Laser Radar Conference, Drexel Univ., Philadelphia, PA (June, 1977).

A. The first paper lays out the principles and detailed results on using "temperature insensitive" H_2O lines for lidar probing via the differential absorption (DIAL) method. Altitude variations of H_2O absorption cross sections, and their effect on lidar returns, are considered. For wavelengths in the range 720-740 nm, explicit predictions are made of the measurement errors to be expected for $[H_2O]$, given certain operating parameters* of the H_2O DIAL system at NASA-Langley Research Center.

Three graphs are given showing $[H_2O]$ measurement accuracy at sea level as a function of distance, for 3 Joules of optical energy, in both vertical and horizontal sounding cases. Good horizontal measurements with 150 meter range resolution can be made out to 5 km; the vertical sounding cases are

*Currently the predicted errors are much more favorable, because a dye amplifier has been added to the system, to give roughly a 200 mJ pulse output.

more problematical because of the falloff with height of both the aerosol backscatterers and the density of water vapor. Optimization for a given range is discussed, principally in terms of the choice of absorption line strength relative to desired range and range resolution. Satisfactory vertical soundings up to 2.5 - 3.5 km are illustrated. Representative curves are given which indicate how the choice of the best H_2O line follows from radiative transfer parameters.

The results given in this paper are directly applicable to lidar measurements that can be carried out at these wavelengths and accumulated optical pulse energies.

B. The second paper carries through several detailed DIAL simulations for $[H_2O]$ measurement using lines in the $\rho\sigma\tau$ bands around 940 nm. The greater line strength permits lower concentrations of H_2O to be detected, so that dye lasers operating at these wavelengths need to be assessed for measurements in the stratosphere as well as the troposphere.

One graph is given for nadir viewing from the Space Shuttle, showing the predicted accuracy in measurements of $[H_2O]$ as a function of altitude. For range cells in the 2 - 5 km range, acceptable DIAL measurements can be carried out up into the lower stratosphere. The choice of different lines is very important, owing to the wide range of line strengths and atmospheric absorption of the on-line signal.

Operation of a balloon-borne, downward looking lidar system at 30 km is indicated in another graph, which predicts extremely good accuracy in $[H_2O]$ up to 15 km altutide, and better than 20% accuracy 10 km below the balloon. Currently the state-of-the-art of H_2O measurements in the stratosphere is such that carrying out frequent and reliable measurements having accuracies of order 25% would be a significant contribution.

Lastly, a Table indicates the measurement errors on $[H_2O]$ for horizontal lidar observations within the stratosphere at 20 and 30 km altitude, assuming extremes of water vapor abundance of 2 ppm (low) and 10 ppm (high). Except for the case of the lowest abundance at the highest altitude, the measurement errors are less than 15% for the range cells within 10-15 km of the balloon. This means that excellent averaged measurements of $[H_2O]$ in the nearby environment can be made using a balloon lidar, without the concern for contamination effects that naturally arises with a local sampling device.

C. The third paper explores the potential of two-color lidar systems for distinguishing between aerosols and molecules by means of optical backscatter observed from an orbital platform. For simplicity, the two colors in question are assumed to be a laser fundamental (e.g., 694.3 nm for ruby) and the single harmonic pulse obtained by means of a frequency doubling crystal (e.g., at 347.2 nm for ruby). Since the Rayleigh scattering from molecules is proportional to λ^{-4}, while aerosol scattering goes roughly as λ^{-1} in the visible, the red-to-blue ratio between the two lidar returns will be a good indicator of aerosol abundance.

This effect is particularly striking in Figure 2 of the paper which shows the altitude-resolved, red/blue lidar "returns ratio" associated with a diffuse aerosol layer which has been added to a standard clear atmosphere model. A real time display of this type, if made available to an astronaut operating the lidar in the Space Shuttle, would give excellent and immediate characterizations of the aerosol structure of the atmosphere beneath the Shuttle. A "real world" example apropos of aerosol layers is the transport of Sahara dust across the Atlantic Ocean to Florida and Cuba; the lidar

technique would permit the observation of altitude profiles which supplement the haze photographs taken by meteorological satellites.

The characterization of simple atmospheric situations is illustrated in Figure 1 of the paper, for which the red/blue returns ratio has been normalized to unity at 10 km (a reasonably clean zone in the atmosphere). An astronaut-compatible display of this type would clearly show major differences in aerosol models of the observed atmosphere. Rough indications of water vapor could also be obtained, by temperature-tuning the 694.3 ruby line onto the H_2O absorption line at 694.3806 nm. It would be hard to determine $[H_2O]$ more accurately than about 25% by these means.

The great difference between the standard "clear" and purely molecular atmosphere cases may hold some interest for the polar atmospheric regions of the earth, which are only very sparsely covered with ordinary meteorological observing stations, and where the aerosol abundance is intimately connected with precipitation and hence with atmospheric scavenging.

Lastly, in this paper we observed that perhaps it will be new types of lasers that make for optimal two-color lidar operation, owing to the relative inefficiency of ruby lasers for use in space and the low quantum yield of photomultipliers at the Nd:YAG fundamental. A candidate laser is Er:YLF which lases at 850 nm (SHG at 425 nm) and is currently being marketed by Sanders Associates (Nashua, NH). Given a rapid engineering development of this system, it could be very good for two-color lidar, because the fundamental is efficiently PM-detectable and the laser can, like Nd:YAG, operate at a high pulse repetition frequency.

Work continues on the inversion of two-color lidar returns, to establish limits on the conclusions to be drawn on the altitude profile of the aerosol size distribution. It is likely that several simultaneous lidar pulses will

be needed for observations of this type, making use of polarization changes and a range of wavelengths covering somewhat more than a factor of two between the extremes.

4. Acknowledgments

The authors wish to express their appreciation to G. Schwemmer for his work on lidar simulations and to M. Morris for his work on the tunable dye laser. The support and encouragement of L. Caudill of the Goddard Space Flight Center is gratefully acknowledged.

Appendix 1: Properties of Dye Solutions

Several practical problems arise in the use of the DTDC-DMSO combination as the dye solution for this laser. The first of these problems relates to photochemical stability of the dye. Whereas the dye efficiency is only slowly eroded by lasing action, a more significant photolytic action results from exposure of the solution to fluorescent room lights. We surmise that this photolysis results from the ultraviolet component of the room lights and have successfully countered the degradation by using ultraviolet-opaque substances in the dye circulating system, and by storing dye solutions in a dark place.

A second set of difficulties arises from the dependence of the dye laser output on temperature. In general, the lasing efficiency of DTDC drops off slowly as temperature increases. However, a lower limit to dye laser operation is set by the freezing point of DMSO at 63°F. We have found that an inadvertent freezing of the dye solution by a dip in room temperature effectively renders the solution useless even after thawing. Optimally the temperature should be maintained at about 70°F.

The biological properties of DTDC are not well studied, but in sufficient dosage it may well be toxic.[1] The toxicity problem in handling dye solutions is complicated by the use of DMSO as a solvent, since DMSO readily diffuses through the skin, transporting solute molecules with it. It is therefore important that any skin contact with dye solutions be avoided, and that gloves be worn as a minimum precaution whenever dye solutions are handled.

[1] Kues, H. A., Lutty, G. A., Laser Focus, 11, No. 5, 59 (May 1975).

Appendix 2

Abstracts of papers cited in Section 3 on lidar simulations for aerosols and water vapor.

NRL Memorandum Report 3430

Proceedings on a Workshop on Remote Sensing of the Marine Boundary Layer

Vail, Colorado

9–11 August 1976

LOTHAR H. RUHNKE,
Editor

Atmospheric Physics Branch
Ocean Sciences Division

June 1977

NAVAL RESEARCH LABORATORY
Washington, D.C.

WATER VAPOR LIDAR TECHNIQUES BELOW 1 MICRON WAVELENGTH

G. Schwemmer & T. Wilkerson

Institute for Physical Science and Technology
University of Maryland, College Park, Maryland 20742

Water vapor profiles in the atmosphere can be obtained from lidar operation in the near-visible wavelengths below 1 micron. Aspects of this capability are discussed here, and a joint experiment of this type with NASA-Langley Research Center is described in another paper at this meeting.[1] Water vapor line spectra between 0.6 and 1.0 μ have previously been summarized[2] with the lidar application in mind.

The differential absorption lidar method is very effective because narrow-band, stable, tunable dye lasers[3] can be tuned to the center of H_2O lines so as to take full advantage of the line strength. For measurements of atmospheric $[H_2O]$ it is important that the line center absorption cross sections, σ_o, depend on temperature as little as possible. The energy levels for temperature-insensitive lines of H_2O are indicated in Figure 1. For atmospheric profiling near 300°K, for example, energy levels 200-250 cm^{-1} most nearly conform to $\partial\sigma_o/\partial T = 0$.

---

*Research supported in part by NASA-GSFC grant NSG-5062 and NASA GSFC Contract No. NAS-5-22527.

[1] B. Northam and E. Browell, paper III.5.

[2] R. Ellingson, T.J. McIlrath, G. Schwemmer and T.D. Wilkerson, "Water Vapor Lidar", Univ. of Md. Tech. Note BN-816, Jan. 1976.

[3] T.J. McIlrath and T.D. Wilkerson, "Status Report on Water Vapor Lidar, Univ. of Md. Tech. Note BN-830 (Jan. 1976).

Figure 2 shows the altitude dependence of σ_o for a number of H_2O lines which have already been selected for temperature-insensitivity. The wavelengths and strengths are based on research in progress at Kitt Peak.[4] Such data are essential for feasibility calculations of H_2O lidar operation from aircraft, and for altitude profiling of H_2O from sea level. The atmospheric models referred to in this paper are those adopted by McClatchey et al at AFCRL.[5]

Calculated lidar returns are shown in Figure 3, for the LaRC/Maryland laser system prior to addition of an amplifier. Off-line returns (detected photons) are predicted to be of order 10^4 per 3 μsec range gate even from 8 km altitude, while the on-line returns can be greatly attenuated by H_2O absorption. The increase of σ_o with altitude yields greater attenuation (solid lines) than in the case of constant cross sections (dashed lines). The correct interpretation of these returns in terms of $[H_2O]$ clearly requires accounting for the altitude effect.

Accuracy of the H_2O lidar occupies much of our attention in the remainder of the paper. Because of the logarithmic derivative occuring in the expression for $[H_2O]$ as a function of the lidar returns, the error propagation of signal and background noise has to be considered in detail, as has been discussed by Schotland.[6]

---

[4] J.W. Brault and W.S. Benedict, private communication.

[5] R.A. McClatchey, R.W. Fenn, J.E.A. Selby, F.E. Volz and J.S. Garing, "Optical Properties of the Atmosphere (Third Edition)", AFCRL-72-0497 (August 1972).

[6] R.M. Schotland, "Errors in the Lidar Measurement of Atmospheric Gases by Differential Absorption", Journal of Applied Meteorology Vol. 13, pp. 71-77 (Feb. 1974).

Figure 4 shows the total error in $[H_2O]$ for a given H_2O line, as a function of altitude for the LaRC/Maryland simulation referred to previously. Range resolution (45, 150, 450 M) is a parameter for the three pairs of curves shown in the Figure. $[H_2O]$ accuracy improves with increasing range cell because of increased H_2O absorption across the length of the cell. We expect the performance of the system currently under test at NASA-Langley to surpass these predictions because of the greater laser pulse energies now available.[1]

For possible maritime applications, we have assumed 3 Joules of tunable, near infrared laser energy - a reasonable figure for shipboard operation in the very near infrared. Figure 5 shows the accuracy in $[H_2O]$ expected for horizontal ranging using the indicated line of H_2O. Out to 4 km range, one can obtain ~ 6% accuracy in $[H_2O]$ even under daylight illumination conditions. The contributions of various error sources are shown, including the "White cell" error if one were to use a calibrating absorption chamber in parallel with the lidar telescope (as in the LaRC/Maryland system).

As noted in Figure 2, much stronger H_2O lines (than the one treated in Figure 5) could be used; however any attendant increase in $[H_2O]$ accuracy would be confined to shorter ranges. The total error curve would upturn sharply nearer the lidar station, because of the greater integrated absorption along the path and the consequent increase of noise in the on-line signal.

Figure 6 and 7 indicate the choices available to the lidar engineer, by virtue of different H_2O line strengths, for the case of vertical sounding from sea level with a 3 Joule, tunable pulse. Figure 6 shows the ~ 5% accuracy in $[H_2O]$ attainable out to 2 km, using one of the lines simulated in Figure 3. To reach higher altitudes with reasonable accuracy, Figure 7 shows the use of a weaker line and a coarser range resolution.

A crucial parameter in such designs is the two-way optical depth, to and from the range of interest, for the on-line radiation. This can have a wide range of values as already indicated by the absorption coefficients in Figure 2. Figure 8 is more explicit and suggests the variety of integrated optical depths (δ) available in the 7200 Å H_2O band. Aside from considerations of range resolution, the greatest accuracy for differential absorption systems is to be obtained for $\delta \approx 1$. For range resolved, signal-processing-limited measurements, maximum accuracy is obtained out to a range R , when $\delta(R) \approx \ell n\{2P(R)E^2 - 1\}$, where $P(R)$ is proportional to the off-line return signal strength and E is the fractional error in the measurement of $P(R)$; (typically $E = .01$). This coincides with the range at which shot noise becomes greater than signal processing noise, indicated on Fig. 6 by an asterisk.

We conclude that dye laser operation and the strength of the H_2O spectrum in the very near infrared are consistent with determination of range-resolved $[H_2O]$ to within a few percent, to ranges of a few kilometers, using the differential absorption method. Ample line strength is available in the 7200, 8200 and 9400 Å bands of H_2O. The required lidar pulse energies are available by means of dyes pumped by solid state lasers (ruby, doubled Nd: YAG) in various oscillator-amplifier configurations.

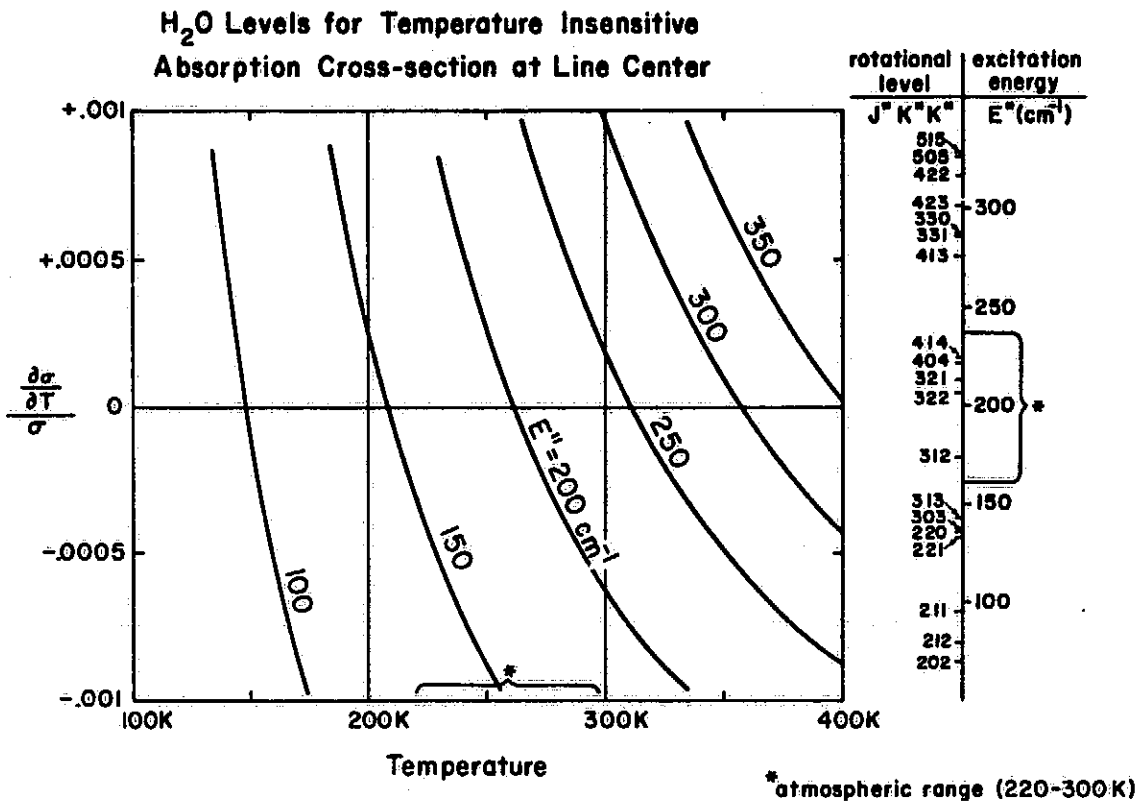

Fig. 1.

Altitude Dependence of
Line-center Absorption Cross-sections,
for Representative H_2O lines,
[Midlat. Summer Atmos. Model]

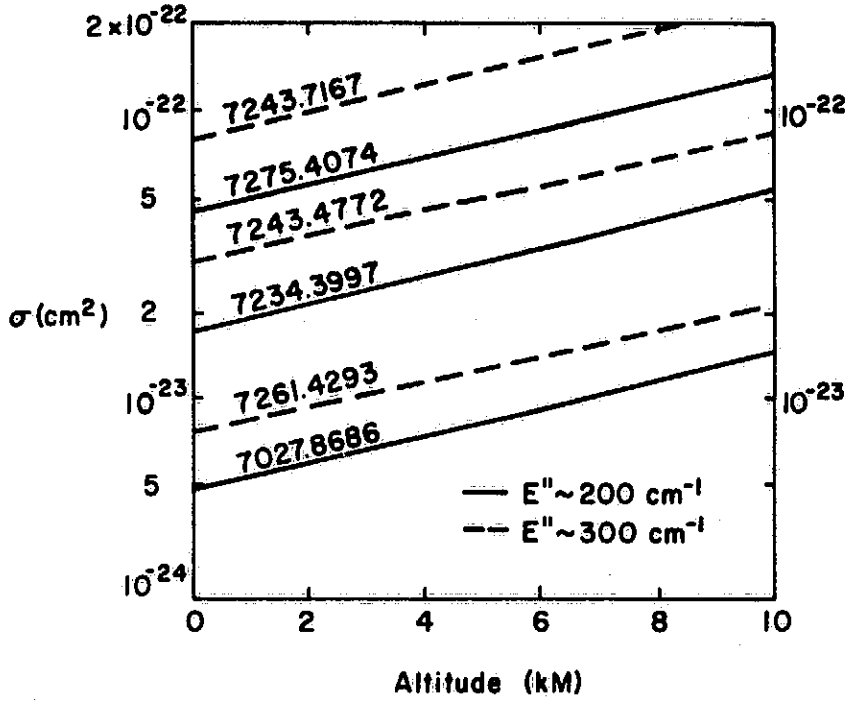

Fig. 2.

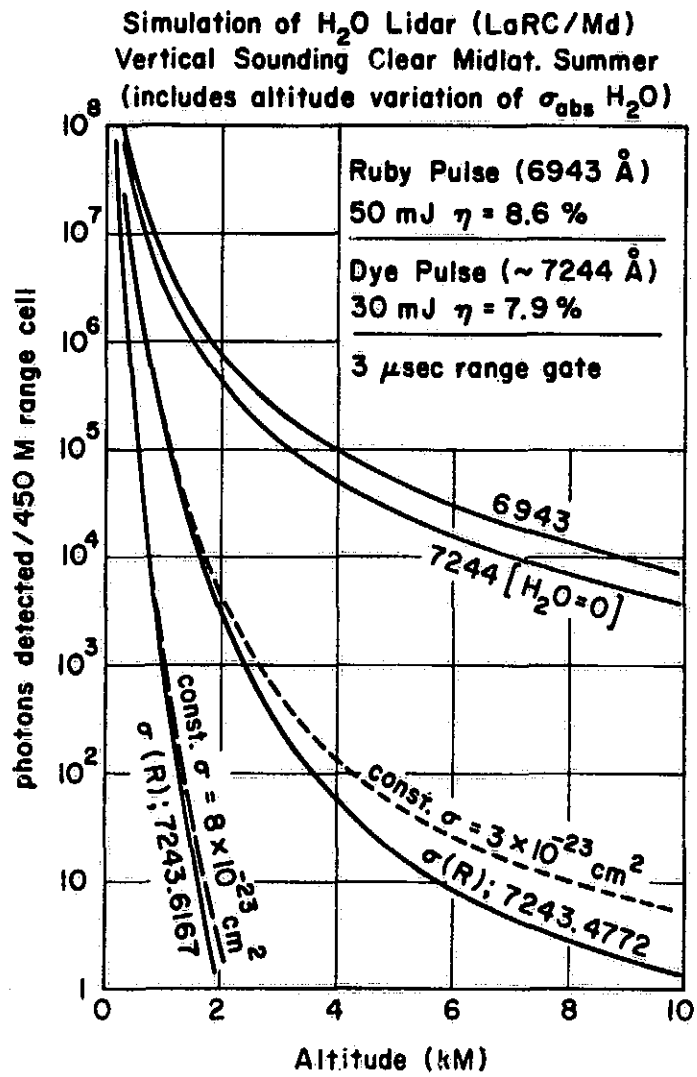

Fig. 3

ORIGINAL PAGE IS
OF POOR QUALITY

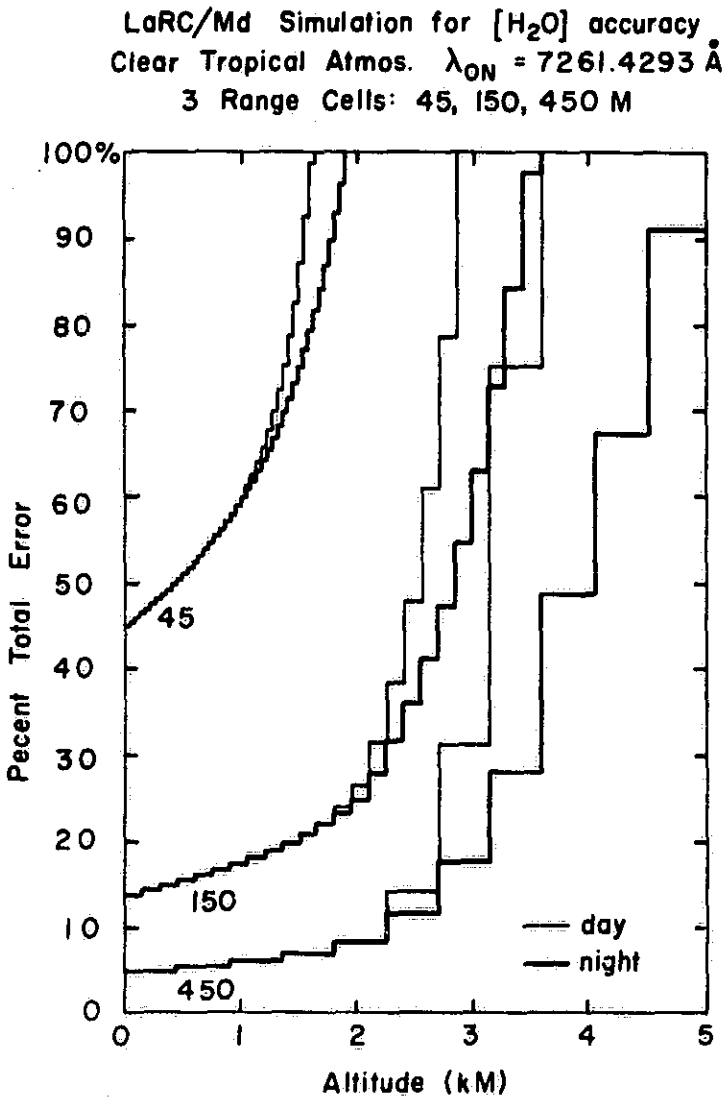
LaRC/Md Simulation for [H2O] accuracy
Clear Tropical Atmos. λON = 7261.4293 Å
3 Range Cells: 45, 150, 450 M
Pecent Total Error
100%
90
80
70
60
50
40
30
20
10
0
45
150
450
day
night
0
1
2
3
4
5
Altitude (kM)

Fig. 4.

SHIPBOARD-COMPATIBLE LIDAR: $[H_2O]$ ACCURACY VS. RANGE
HORIZONTAL RANGING AT SEA LEVEL, CLEAR TROPICAL ATMOSPHERE

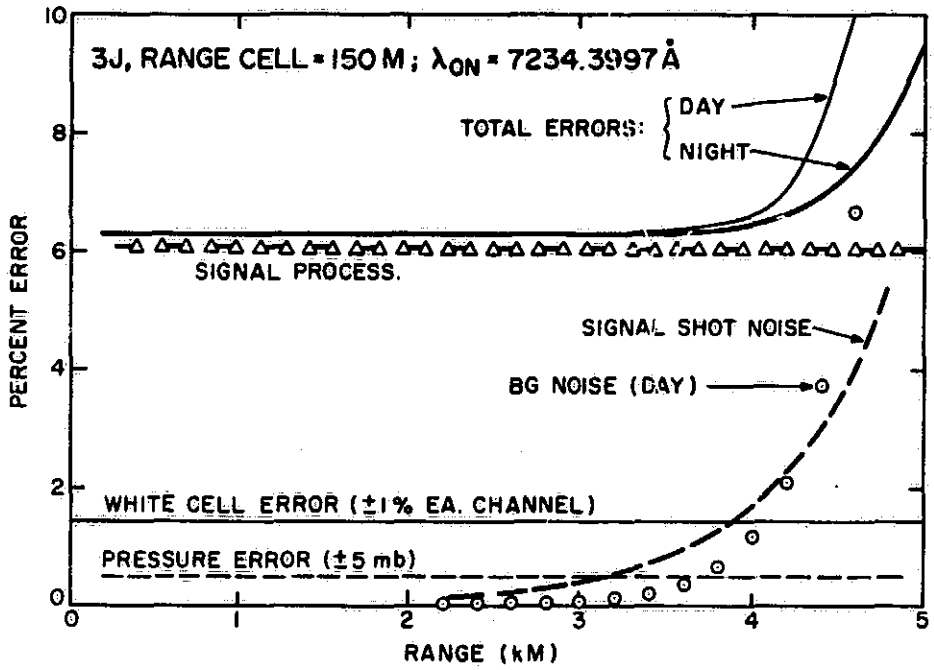

Fig. 5.

SHIPBOARD-COMPATIBLE LIDAR: $[H_2O]$ ACCURACY VS. ALTITUDE
VERTICAL RANGING FROM SEA LEVEL (2 kM OPTIMIZATION)
CLEAR, TROPICAL ATMOSPHERE

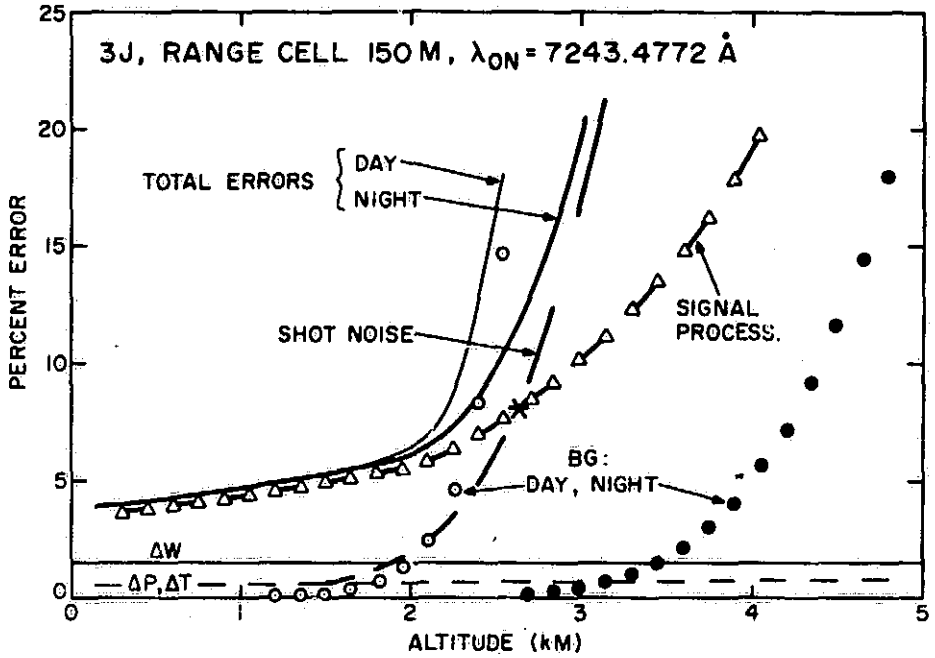

Fig. 6.

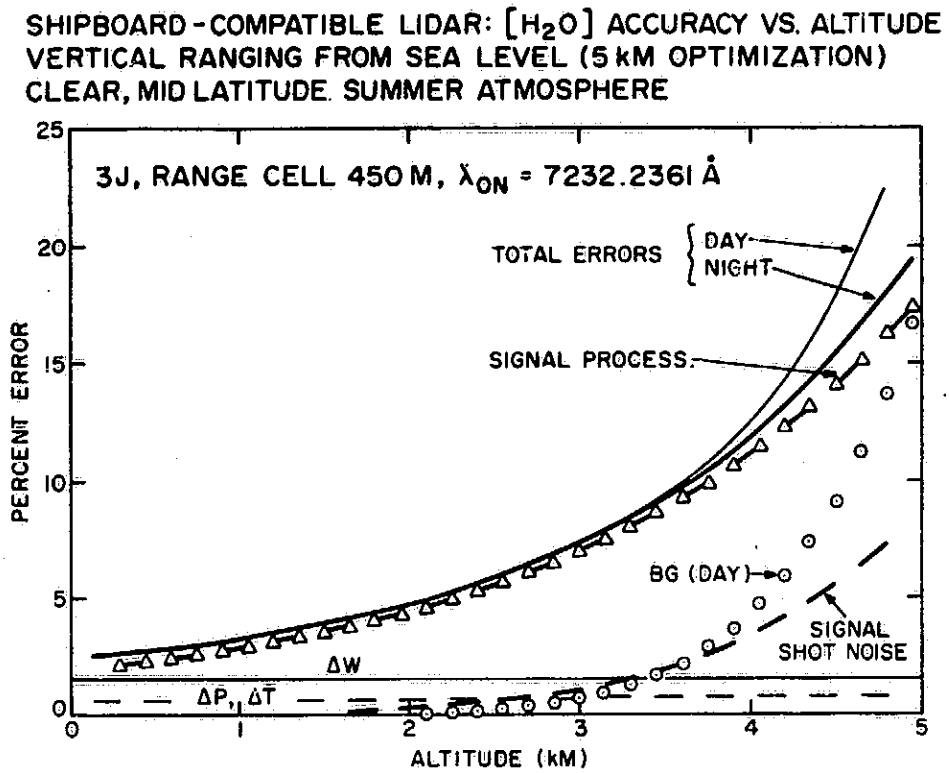

Fig. 7.

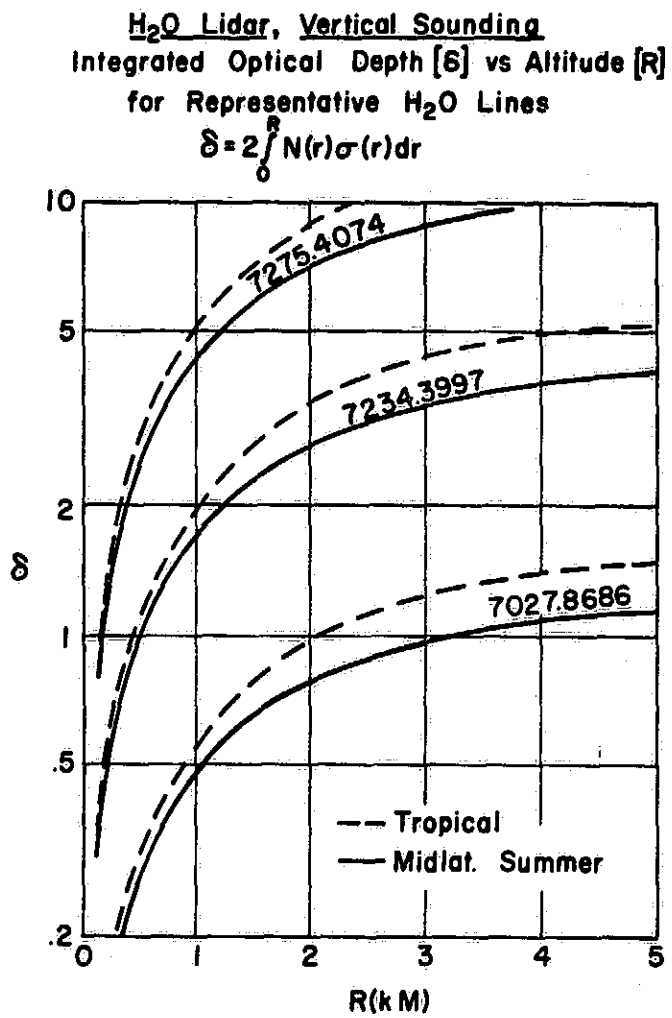
H2O Lidar, Vertical Sounding
Integrated Optical Depth [δ] vs Altitude [R]
for Representative H2O Lines
δ = 2∫0R N(r)σ(r)dr
10
5
2
1
.5
.2
δ
7275.4074
7234.3997
7027.8686
Tropical
Midlat. Summer
0
1
2
3
4
5
R(k M)

Fig. 8.

CONTRIBUTIONS FROM

UNIVERSITY OF MARYLAND
Division of Mathematical and Physical Sciences and Engineering

Institute for Physical Science and Technology
Space Sciences Building
College Park, MD 20742

-2702
Tel: (301) 454-3440

TO :

8th INTERNATIONAL

LASER RADAR CONFERENCE

Sponsored by:

COMMITTEE ON LASER ATMOSPHERIC STUDIES
AMERICAN METEOROLOGICAL SOCIETY

in COOPERATION with

OPTICAL SOCIETY OF AMERICA
NASA LANGLEY RESEARCH CENTER

CONFERENCE ABSTRACTS

June 6th through 9th, 1977
DREXEL UNIVERSITY
Philadelphia, Pennsylvania

WATER VAPOR LIDAR AT 9400 Å: ATMOSPHERIC OBSERVATIONS FROM ORBITAL AND STRATOSPHERIC PLATFORMS*

by

G. Schwemmer and T. D. Wilkerson
Institute for Physical Science and Technology
University of Maryland, College Park, Maryland 20742

Numerical simulations of differential absorption lidar in the 9400 Å water vapor bands have been made to define future experiments and determine their limitations. Orbital platforms such as the Space Shuttle are preferable for global mapping of atmospheric water vapor, while stratospheric platforms offer more accurate measurements within local regions of order 5-20 kM in size. Many of the 9400 Å H_2O lines are strong enough for absorption detection of H_2O above 8 kM, and these same bands also contain weaker lines which are more appropriate for observations at low altitude where the H_2O abundance is high. This paper extends our previous reports[1,2] on water vapor lidar in the 7200 Å region where the line strengths are in this weaker category.

Figure 1 shows the predicted accuracy of H_2O profiling from 200 kM altitude under the assumptions cited on the graph. Three cases are treated, in which the absorption line strength for the "on-line" channel makes the main difference. The accuracy for the weakest line degrades at high altitude because of low H_2O absorption across the given range cell. For stronger lines, the low altitude accuracy for $[H_2O]$ is due to extinction of the on-line signal. To construct a reasonably continuous $[H_2O]$ profile, a set of such measurements would be made; these calculations show that the 9400 Å lines have a sufficiently wide range of strengths to carry the work well into the stratosphere. This type of lidar system would complement the higher altitude atmospheric profiling currently planned for orbital passive IR systems.

Figure 2 displays the accuracies in $[H_2O]$ obtainable with downward ranging from 20 kM altitude, using the same assumptions as in Fig. 1. The high accuracy "trough" for each case of line strength is much wider than

*Research supported in part by NASA-Goddard Grant No. NSG-5062 Sup. 1 and Contract No. NAS-5-22537, and by the University of Maryland.

in the orbital situation; the three lines employed here would suffice for complete profiling from the ground to the transmitter altitude.

Horizontal ranging within the stratosphere calls for a different approach. Range cells of 5-10 kM are needed for sufficient absorption, and the maximum lidar range will usually be about 15-25 kM owing to low backscatter efficiency. Accurate measurement of average water vapor concentration within 10 kM of the laser is possible. This may be very useful in establishing the local state of chemical equilibrium in the stratosphere, given the simultaneous observation of other species such as OH, O_3, NO and NO_2.

Table 1 summarizes results for horizontal observations of H_2O at 20 and 30 kM altitude. The range of 2-10 ppm mixing ratio was adopted from in situ measurements having experimental errors of order 30%. A water vapor lidar operated in this fashion offers substantial improvements in accuracy over present methods of measuring stratospheric H_2O. In this case it is not so much a "remote sensor" as a high rep. rate monitor of the nearby average environment, out to distances 1000-10000 times the size of the region which might be contaminated by the requisite aircraft or balloon platform.

References

1. Schwemmer, G. and T. D. Wilkerson, 1976: Water Vapor Lidar Techniques Below 1 Micron Wavelength, Proceedings of Navy Remote Sensing Conf. Vail, Colorado, (August, 1976).
2. Ellingson, R. et al., 1976: Water Vapor Lidar, Univ. of Maryland Tech. Note BN-816.
3. Chaloner, H. K., 1975: Stratospheric Measurements of H_2O and the Diurnal Change of NO and NO_2, Nature, 258, Dec. 25, pp. 696-7.
4. Harries, J. E., et al., 1973: Measurements of the Submillimetre Stratospheric Emission Spectrum from A Balloon Platform, Infra. Phys. 13, 149-155.
5. Mastenbrook, H. J., 1971: The Variability of Water Vapor in the Stratosphere, J. Atmos. Sci. 28, 1495-1501.

TABLE I

Accuracy in Stratospheric H_2O Measurements

Altitude	ppm	mg/kg	$10^{12}/cm^3$	% error
20 km	$2.0 \pm .3$	$1.24 \pm .17$	$3.7 \pm .5$	13.8
	10.0 ± 1.4	$6.2 \pm .3$	$18.7 \pm .9$	4.7
30 km	2.0 ± 1.2	$1.24 \pm .73$	$.66 \pm .39$	59.
	10.0 ± 1.2	$6.2 \pm .8$	$3.3 \pm .4$	12.5

H_2O line λ 9374.057 Å:

Line center absorption cross section $=$ 2.04×10^{-20} cm^2 @ 20 kM

Line center absorption cross section $=$ 2.59×10^{-20} cm^2 @ 30 kM

WATER VAPOR LIDAR: $[H_2O]$ accuracy, Space Shuttle 3J, λ - 9400Å; clear midlatitude summer night

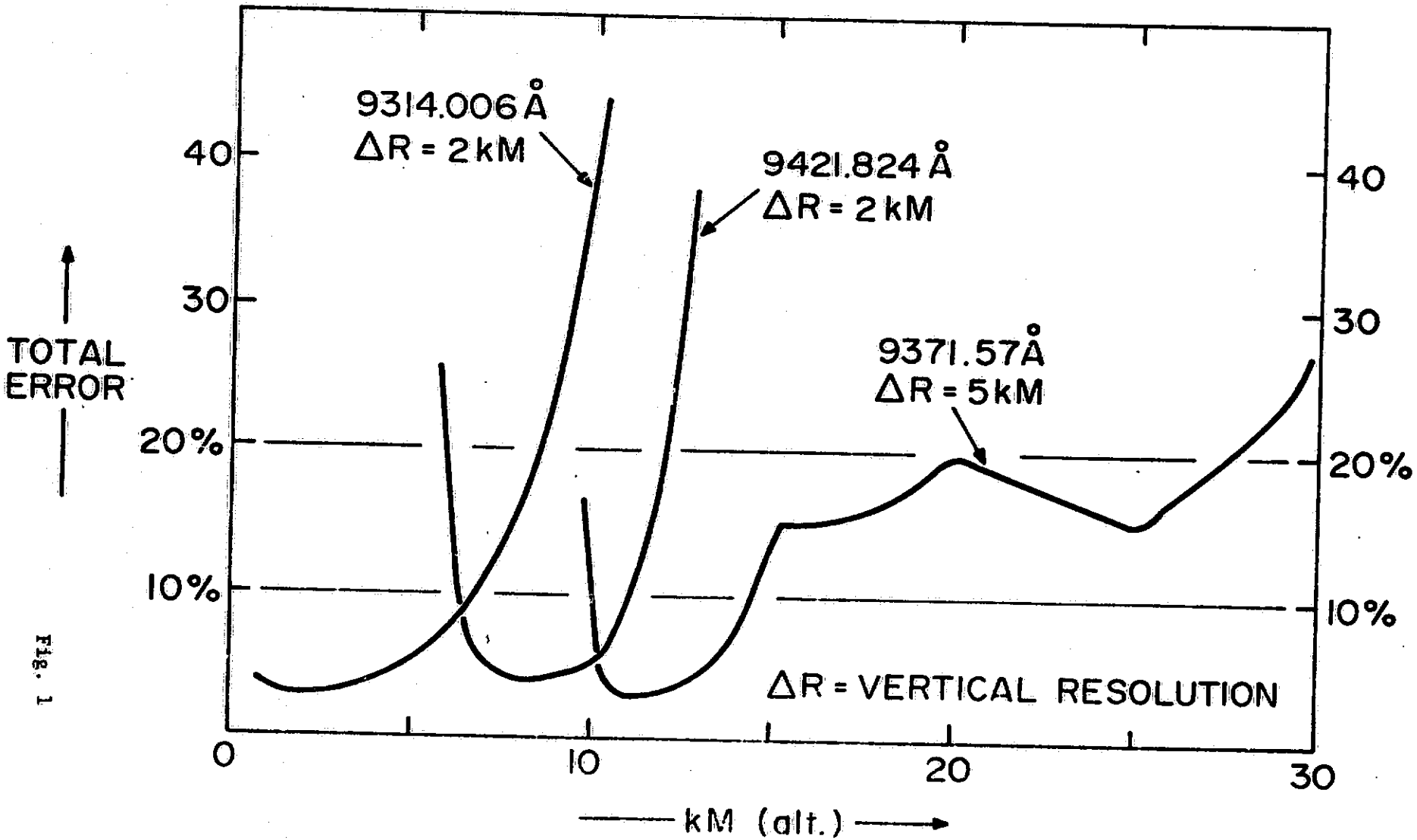

Fig. 1

WATER VAPOR LIDAR at 30kM: $[H_2O]$ accuracy vs. altitude
clear, midlat. summer night; 3J, 2kM vertical resolution

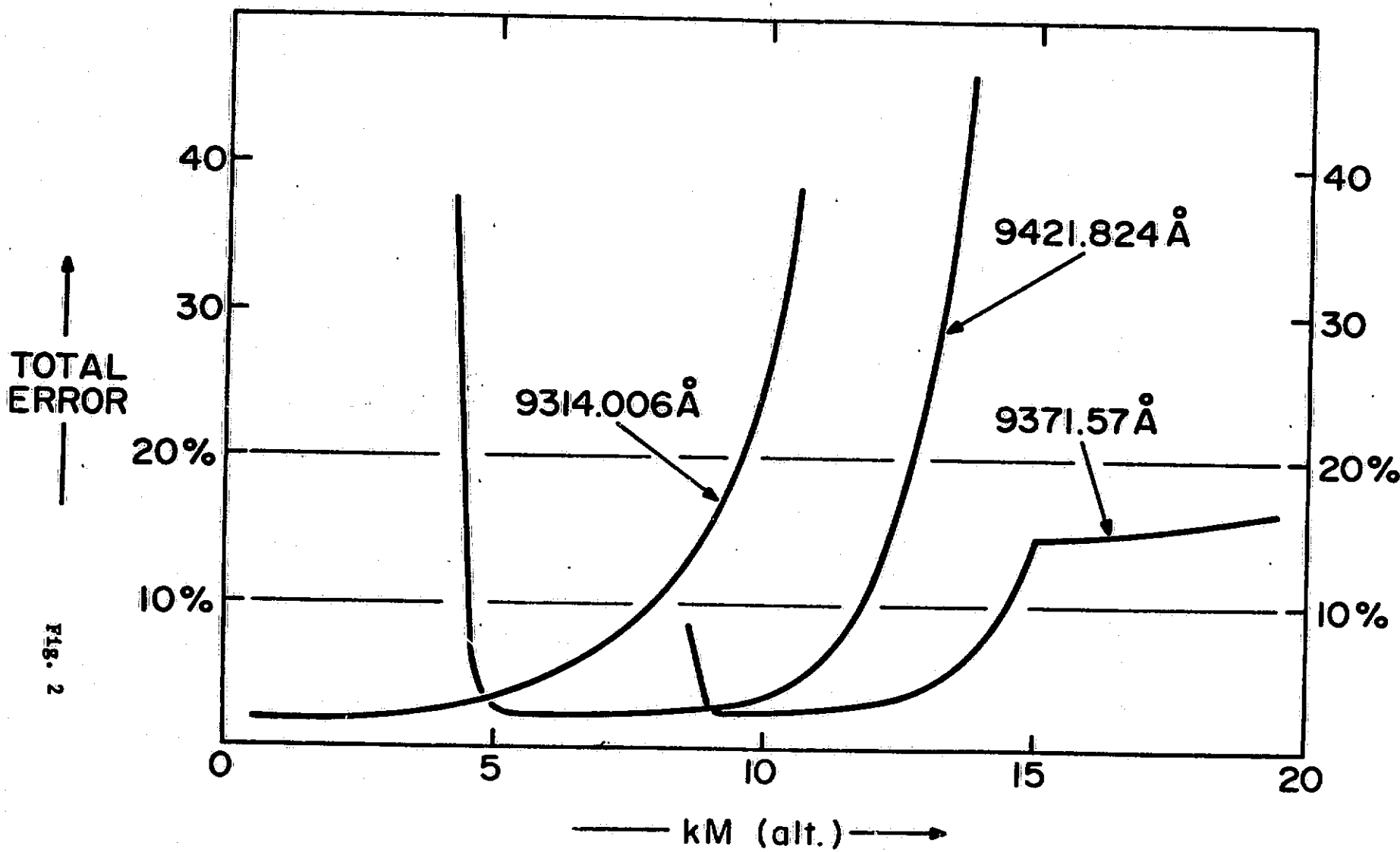

Fig. 2

TWO-COLOR ATMOSPHERIC LIDAR FOR SPACE SHUTTLE OBSERVATIONS OF MOLECULAR AND AEROSOL BACKSCATTER*

by

T. D. Wilkerson and G. Schwemmer
Institute for Physical Science and Technology
University of Maryland, College Park, Maryland 20742

Space shuttle feasibility is demonstrated for two-color, visible lidar observations of atmospheric backscatter, primarily to distinguish between aerosol and molecular constituents. Aerosol layers are shown to be measurable via the lidar return ratio between the laser fundamental and its frequency-doubled radiation. In addition such instruments are technically interesting in the evolution of space borne laser systems, because their complexity is intermediate between the single laser and the laser-pumped, tunable dye laser.

The groundwork for two-color lidar has been well laid by McCormick and colleagues in calculations[1] and experiments[2] with ruby/doubled ruby on NASA-Langley's 48-inch system.

The ruby laser case (6943 Å/3472 Å) is calculated here for a Space Shuttle platform at 200 kM altitude viewing the atmosphere at nadir. A real-time data display is proposed (Fig. 1) that may also enable an astronaut-observer to make rough distinctions between atmospheric humidity conditions as well as aerosol abundance. (This would require temperature-tuning of the ruby fundamental to the nearly H_2O absorption line λ 6943.806). The most striking feature of the ruby case is the capability of the red-to-blue ratio of lidar returns for the profiling of aerosol layers (e.g., see Fig. 2).

*Research supported in part by NASA-Goddard Grant No. NSG-5062 Sup. 1 and Contract No. NAS-5-22537, and by the University of Maryland.

Disadvantages of both the standard ruby and Nd:YAG systems for the Shuttle are cited, namely: low laser efficiency and pulse rep. rate for ruby, and low detection efficiency for the YAG fundamental (1.06 μ). Remsberg and Northam have calculated[3] that this latter radiation is not very useful for aerosol studies from orbit.

As an alternative we suggest the relatively new laser material Er:YLF (~ 8500 Å; doubled to 4250 Å) on the grounds of laser efficiency combined with photomultiplier detection of both the doubled and fundamental radiation. Vertical atmospheric soundings from sea level and from orbit are presented, using simultaneous YLF and doubled-YLF pulses of 1 J and 100 mJ energy respectively. The "red"-to-blue ratio provides good visualization of aerosol profiles in a variety of atmospheric situations including maritime haze.

References

1. McCormick, M. P., "Simultaneous Multiple Wavelength Laser Radar Measurements of the Lower Atmosphere", Proc. Electro-Optics International Conf., Brighton, England; pp. 495-512 (March, 1971).
2. W. H. Fuller, T. J. Swissler and M. P. McCormick, "Comparative Analysis of Red-Blue Lidar and Rawinsonde Data" in NASA CP-2004, Proc. of Meeting on Atmospheric Aerosols: Their Optical Properties and Effects, Williamsburg, Va. (Dec., 1976).
3. Ellis E. Remsberg and G. Burton Northam, "Feasibility of Atmospheric Aerosol Measurements with Lidar from Space Shuttle", in NASA CP-2004, Proc. of Meeting on Atmospheric Aerosols: Their Optical Properties and Effects, Williamsburg, Va. (Dec., 1976).

LIDAR RETURNS RATIO FOR 3 MODEL ATMOSPHERES

SHUTTLE (200 kM) RUBY LASER AND DOUBLED RUBY 6943/3472 NORMALIZED TO UNITY @ 10 kM ALT.

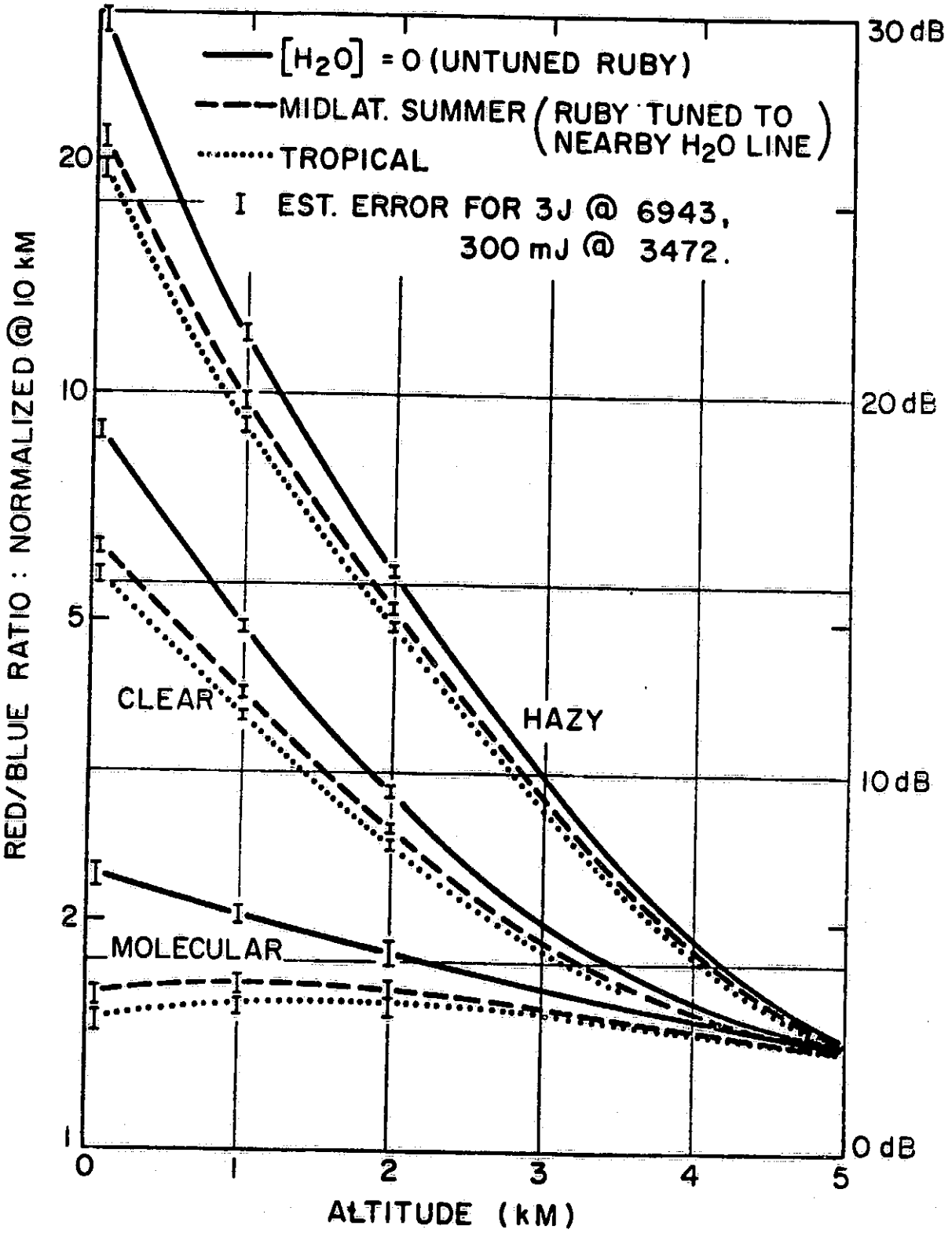

Figure 1

SHUTTLE LIDAR RETURN RATIO (6943/3472)

2 STANDARD ATMOSPHERES AND CLEAR + DUST LAYER

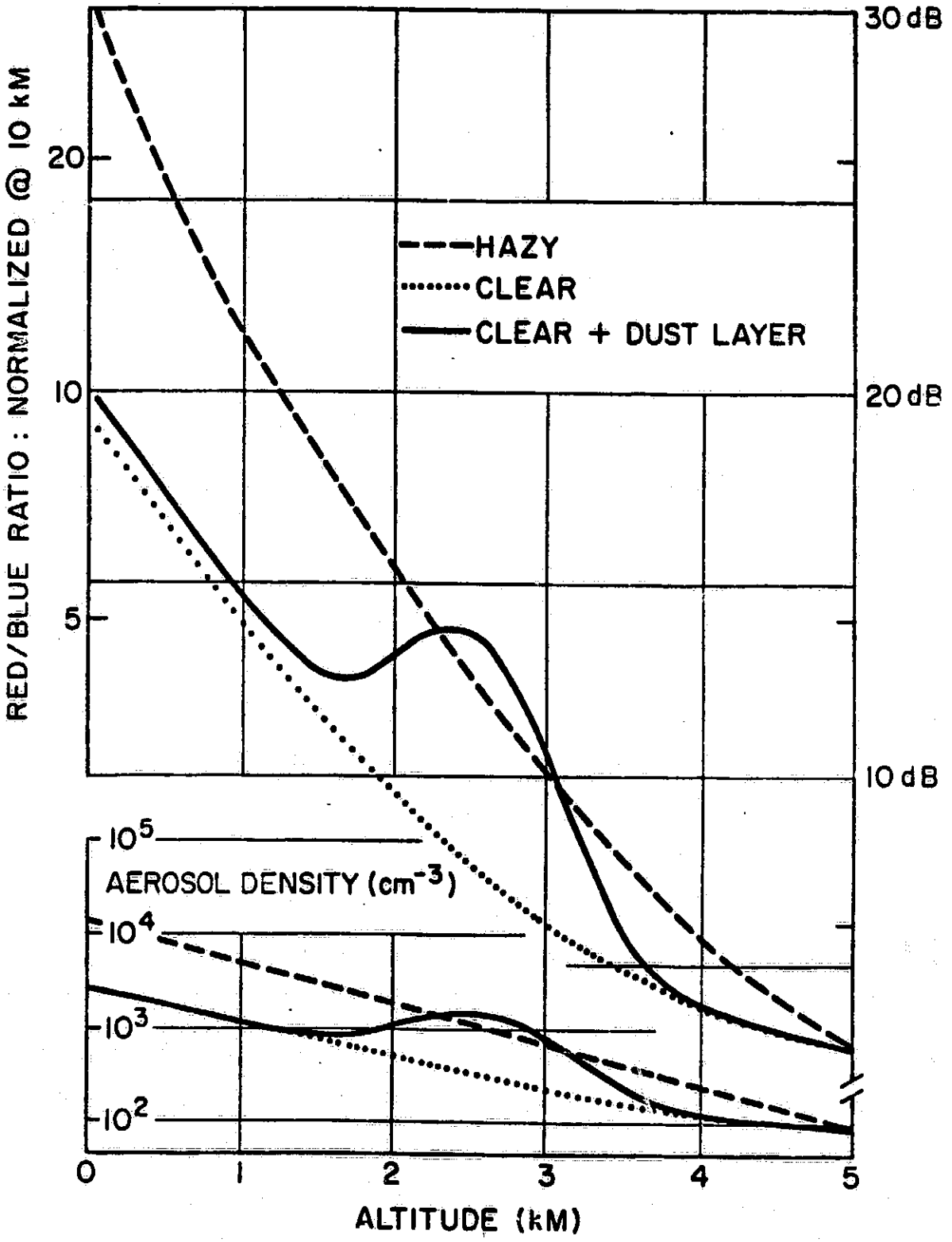

Figure 2

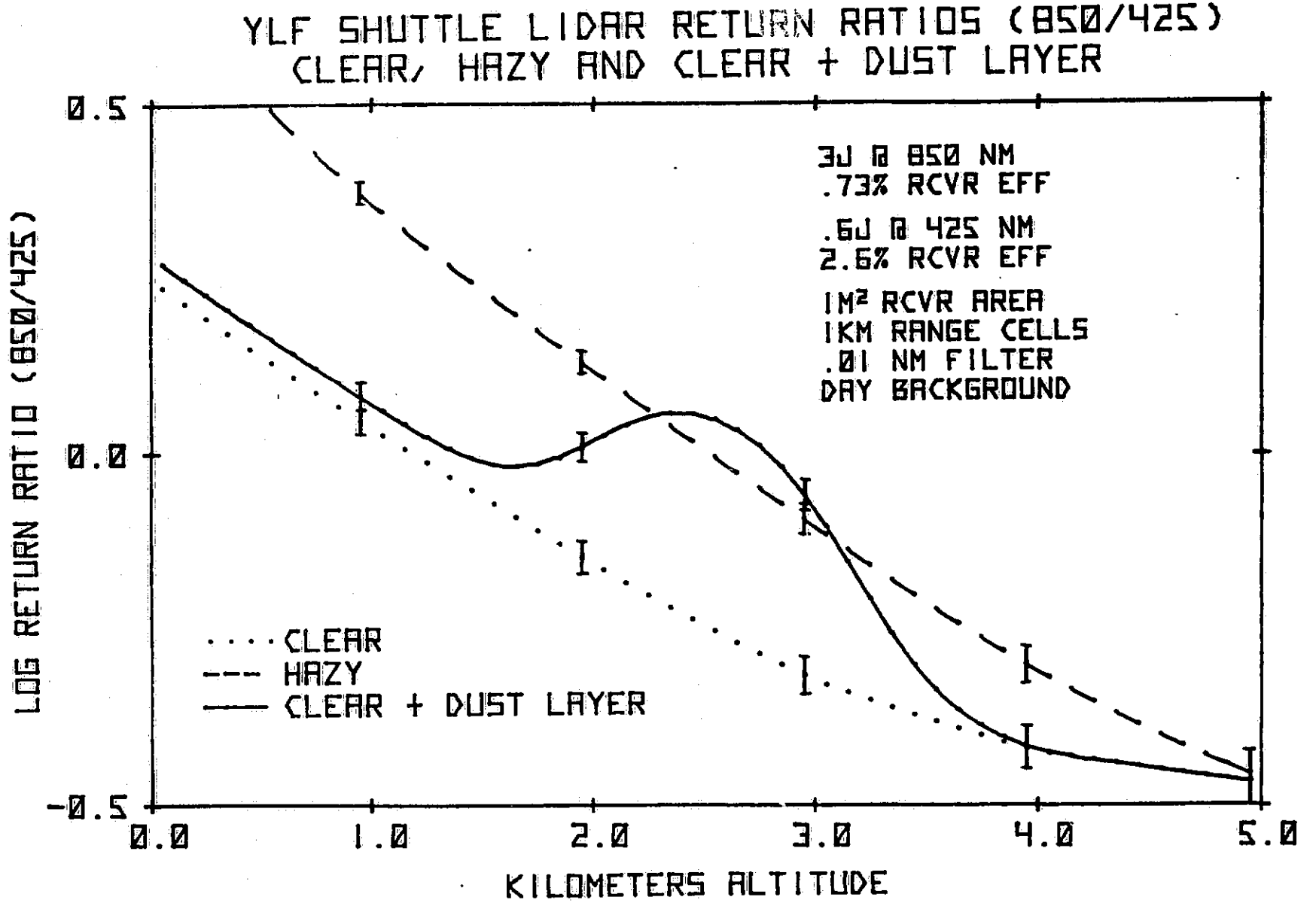

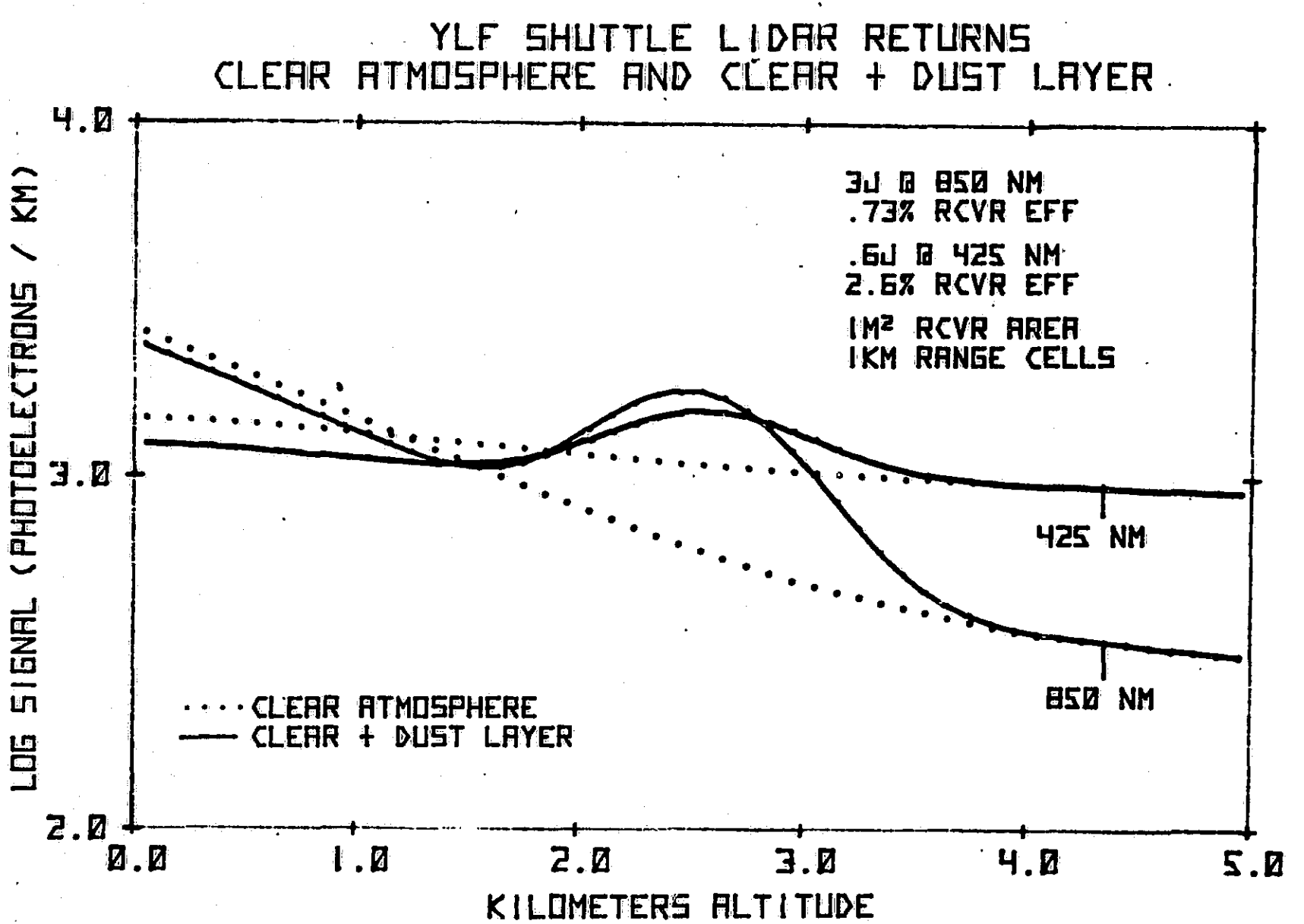
YLF SHUTTLE LIDAR RETURNS
CLEAR ATMOSPHERE AND CLEAR + DUST LAYER
3J @ 850 NM
.73% RCVR EFF
.6J @ 425 NM
2.6% RCVR EFF
1M² RCVR AREA
1KM RANGE CELLS
425 NM
850 NM
CLEAR ATMOSPHERE
CLEAR + DUST LAYER
LOG SIGNAL (PHOTOELECTRONS / KM)
4.0
3.0
2.0
0.0
1.0
2.0
3.0
4.0
5.0
KILOMETERS ALTITUDE